BOUND STATES OF QUANTUM DOTS PROXIMITIZED TO SUPERCONDUCTORS*

T. Domański, R. Taranko

Institute of Physics, M. Curie-Skłodowska University, 20-031 Lublin, Poland

L. Soták, M. Žonda

Faculty of Mathematics and Physics, Charles University
Ke Karlovu 5, 12116 Praha 2, Czech Republic

Received 28 February 2026, accepted 16 March 2026, published online 15 May 2026

We investigate quasiparticle states driven by the proximity effect in the quantum dot(s) coupled to superconducting samples. For the single quantum impurity, we show that its subgap spectrum consists of either the magnetically unpolarized (Andreev) or polarized (Yu–Shiba–Rusinov) bound states appearing at energies which depend on the hybridization strength with a superconductor. We also analyze the molecular bound states of the double quantum dot attached in series to a superconductor and weakly coupled to a metallic lead on the opposite side. For this setup, we show that a magnetic field is detrimental to the on-dot pairings, in much the same way as spinful impurities are pair-breakers for the Cooper pairs in conventional bulk superconductors. Finally, we address the issue of triplet pairing induced by the spin–orbit interactions in superconducting nanostructures.

DOI:10.5506/APhysPolB.57.5-A11

1. Introduction

Impurities are omnipresent in solids and qualitatively affect their properties. In metallic samples, they are responsible for the residual resistivity at low temperatures and, in the case of magnetic impurities, for the logarithmic increase of resistivity associated with the Kondo effect. In semiconductors, donor and acceptor impurities play a pivotal role in controlling charge transport, which underlies numerous technological applications. The role of impurities in superconductors is more subtle. Anderson [1] predicted that a dilute concentration of nonmagnetic impurities does not significantly

* Presented at the Concepts in Strongly Correlated Quantum Matter Conference (CSCQM), Kraków, Poland, 20–22 November, 2025.

affect the critical temperature of conventional isotropic (s-wave) BCS superconductors. In contrast, magnetic scattering centers act as Cooper pair breakers and suppress superconductivity. This behavior differs from unconventional superconductors, such as high-temperature cuprates, where the exchange-interaction driven pairing in real space [2] has been predicted to be enhanced by local inhomogeneities [3].

The remarkable development of scanning tunneling spectroscopy has enabled direct experimental access to the quasiparticle spectra of impurities deposited on the surfaces of conventional [4], unconventional [5], and topologically nontrivial superconductors [6]. Measurements performed on impurities embedded in isotropic BCS-type superconductors have revealed resonant in-gap features associated with impurity-induced bound states [4, 7]. Similar subgap excitations have been observed in quantum dots coupled to superconducting leads, where they appear as the Andreev or Yu–Shiba–Rusinov (YSR) bound states depending on the interaction regime. Comprehensive reviews of these bound states have been given in [8–10]. Currently, intensive activities devoted to such subgap quasiparticle states of superconducting nanohybrids are mainly driven by their perspectives for the advancement of quantum information technology [11, 12].

Furthermore, from the point of view of fundamental physics, the superconducting nanostructures can be regarded as a convenient platform for investigating a competition between the local pairing and strong correlation effects [13]. These phenomena are empirically detectable via the tunneling conductance, which in the subgap regime is dominated by the electron-to-hole (Andreev) scattering processes. Such measurements have been done for quantum dots in two-terminal junctions, using InAs nanoscopic islands [14], carbon nanotubes [15], semiconducting wires [16], *etc.* Other studies have explored three-terminal configurations, comprising two metallic electrodes interconnected through two quantum dots with the superconducting lead. In such a geometry, the Coulomb repulsion combined with the magnetic side-gates [17] efficiently splits the paired electrons from the superconductor into different normal leads, where their quantum entanglement is retained over certain distances. Recent activities focus on the multi-dot [18–20] and/or multi-terminal [21] superconducting structures for engineering the topological states of matter.

In this work, we analyze the formation and evolution of subgap bound states due to electron pairing in quantum dots hybridized with superconducting reservoirs, focusing on the interplay between hybridization strength and magnetic polarization. We first characterize the emergence of impurity-induced in-gap states in the single-dot configuration and identify the parameter regimes governing their spectral evolution. We then extend the analysis to the case of multiple impurities and the evolution of individual

bound states into the formation of molecular-like structures. As a minimal realization of such hybridization effects, we consider a double quantum dot system, which has recently been investigated experimentally using STM [22] and ballistic tunneling spectroscopy [23–25]. Within this setup, we examine the suppression of local BCS-like singlet pairing on the dots following a quench of the magnetic field from zero to a finite value. Finally, we address the emergence of inter-dot triplet correlations in the presence of spin–orbit interaction. We demonstrate that the combined action of Zeeman splitting and spin-mixing tunneling can generate equal-spin pairing components. Such a scenario is considered for the bottom-up construction of topological superconductivity, hosting the poor man's Majorana modes [18–20].

2. Mutation of Andreev to Shiba states

Let us begin by analyzing the subgap states of a single quantum dot coupled to an isotropic superconductor. The system can be described by the Anderson impurity Hamiltonian

$$\hat{H} = \hat{H}_{\mathrm{S}} + \hat{H}_{\mathrm{S-QD}} + \sum_{\sigma} \varepsilon_{\sigma}\, \hat{d}^{\dagger}_{\sigma}\, \hat{d}_{\sigma} + U\, \hat{n}_{d\uparrow}\, \hat{n}_{d\downarrow}\,. \tag{1}$$

Here, $\hat{d}_{\sigma}$ ($\hat{d}^{\dagger}_{\sigma}$) are the annihilation (creation) operators of electrons with spin $\sigma = \uparrow, \downarrow$, the energy level denoted by ε_{σ} can depend on spin, U is the potential of on-dot repulsion between the opposite-spin electrons, and $\hat{n}_{d\sigma} = \hat{d}^{\dagger}_{\sigma}\hat{d}_{\sigma}$ stands for the number operator. The superconductor can be described by the effective BCS-type Hamiltonian $\hat{H}_{\mathrm{S}} = \sum_{\boldsymbol{k},\sigma} \xi_{\boldsymbol{k}\mathrm{S}} \hat{c}^{\dagger}_{\boldsymbol{k}\sigma\mathrm{S}} \hat{c}_{\boldsymbol{k}\sigma\mathrm{S}} - \sum_{\boldsymbol{k}} \Delta \left(\hat{c}^{\dagger}_{\boldsymbol{k}\uparrow\mathrm{S}} \hat{c}^{\dagger}_{-\boldsymbol{k}\downarrow\mathrm{S}} + \hat{c}_{-\boldsymbol{k}\downarrow\mathrm{S}} \hat{c}_{\boldsymbol{k}\uparrow\mathrm{S}} \right)$, where Δ is the pairing gap, and $\xi_{\boldsymbol{k}\mathrm{S}} = \varepsilon_{\boldsymbol{k}\mathrm{S}} - \mu_{\mathrm{S}}$ are energies measured with respect to the chemical potential μ_{S}. The quantum dot is hybridized with a bulk superconductor through the term

$$\hat{H}_{\mathrm{S-QD}} = \sum_{\boldsymbol{k},\sigma} \left(V_{\boldsymbol{k}\mathrm{S}}\, \hat{d}^{\dagger}_{\sigma}\, \hat{c}_{\boldsymbol{k}\sigma\mathrm{S}} + V^{*}_{\boldsymbol{k}\mathrm{S}}\, \hat{c}^{\dagger}_{\boldsymbol{k}\sigma\mathrm{S}}\, \hat{d}_{\sigma} \right) , \tag{2}$$

where $V_{\boldsymbol{k}\mathrm{S}}$ denote the matrix elements. Roughly speaking, they characterize an overlap between wave-functions of the localized QD electrons and the itinerant electrons of the superconductor. In conventional superconductors, the pairing gap is of the order of millielectronvolts, therefore, we restrict our considerations to the low-energy sector, *i.e.* corresponding to the large bandwidth limit $|V_{\boldsymbol{k}\mathrm{S}}| \ll D$ (where $-D \leq \varepsilon_{\boldsymbol{k}\mathrm{S}} \leq D$). Under such conditions, we can treat the coupling strength $\Gamma_{\mathrm{S}} = 2\pi \sum_{\boldsymbol{k}} |V_{\boldsymbol{k}\mathrm{S}}|^2 \delta(\omega - \xi_{\boldsymbol{k}\mathrm{S}})$ as a constant (ω-independent) quantity.

The hybridization term (2) extends the pairing of electrons on the quantum dot, leading to the appearance of quasiparticle states inside the pairing gap of the bulk superconductor. To study their signatures, we proceed within the BCS formalism, introducing the single-particle Green's function $\boldsymbol{G}(\tau,\tau') = \langle\langle\hat{\Psi}(\tau);\hat{\Psi}^\dagger(\tau')\rangle\rangle$ in the Nambu representation $\hat{\Psi}^\dagger = (\hat{d}^\dagger_\uparrow, \hat{d}_\downarrow)$, $\hat{\Psi} = (\hat{\Psi}^\dagger)^\dagger$. Under equilibrium conditions, it depends only on the time difference τ–τ' and its Fourier transform can be expressed as

$$\boldsymbol{G}(\omega)^{-1} = \begin{pmatrix} \omega-\varepsilon_\uparrow & 0 \\ 0 & \omega+\varepsilon_\downarrow \end{pmatrix} - \boldsymbol{\Sigma}^0(\omega) - \boldsymbol{\Sigma}^U(\omega)\,. \tag{3}$$

The self-energy $\boldsymbol{\Sigma}^0$ refers to the hybridization of an uncorrelated quantum dot with the reservoirs, and the term $\boldsymbol{\Sigma}^U(\omega)$ accounts for effects due to the Coulomb repulsion U. The uncorrelated part can be analytically obtained from the Dyson equation [26]

$$\boldsymbol{\Sigma}^0(\omega) = \sum_{\boldsymbol{k}} |V_{\boldsymbol{k}\mathrm{S}}|^2 \; \boldsymbol{g}_\mathrm{S}(\boldsymbol{k},\omega)\,, \tag{4}$$

where the matrix Green's function of the superconductor is given by

$$\boldsymbol{g}_\mathrm{S}(\boldsymbol{k},\omega) = \begin{pmatrix} \omega-\xi_{\boldsymbol{k}\mathrm{S}} & \Delta \\ \Delta & \omega+\xi_{\boldsymbol{k}\mathrm{S}} \end{pmatrix}^{-1}. \tag{5}$$

In the wide bandwidth limit, the self-energy (4) simplifies to

$$\boldsymbol{\Sigma}^0(\omega) = -\frac{\Gamma_\mathrm{S}}{2}\gamma(\omega)\begin{pmatrix} 1 & \frac{\Delta}{\omega} \\ \frac{\Delta}{\omega} & 1 \end{pmatrix} \tag{6}$$

with an ω-dependent function

$$\gamma(\omega) = \begin{cases} \frac{\omega}{\sqrt{\Delta^2-\omega^2}} & \text{for} \quad |\omega| < \Delta\,, \\ \frac{i\,|\omega|}{\sqrt{\omega^2-\Delta^2}} & \text{for} \quad |\omega| > \Delta\,. \end{cases} \tag{7}$$

The quasiparticle excitation energies of the quantum dot are determined by the poles of the dot Green's function $\boldsymbol{G}(\omega)$. For the uncorrelated case ($U \to 0$), the matrix Green's function has the form

$$\boldsymbol{G}(\omega) \;=\; \frac{1}{(\tilde{\omega}-\varepsilon_\uparrow)\,(\tilde{\omega}+\varepsilon_\downarrow) - \left(\frac{\tilde{\Gamma}_\mathrm{S}}{2}\right)^2} \begin{pmatrix} \tilde{\omega}+\varepsilon_\downarrow & -\frac{\tilde{\Gamma}_\mathrm{S}}{2} \\ -\frac{\tilde{\Gamma}_\mathrm{S}}{2} & \tilde{\omega}-\varepsilon_\uparrow \end{pmatrix}. \tag{8}$$

In the subgap regime ($|\omega| < \Delta$), the auxiliary parameters are defined by

$$\tilde{\omega} = \omega + \frac{\Gamma_S}{2}\frac{\omega}{\sqrt{\Delta^2 - \omega^2}}, \tag{9}$$

$$\tilde{\Gamma}_S = \Gamma_S \frac{\Delta}{\sqrt{\Delta^2 - \omega^2}}, \tag{10}$$

whereas outside the pairing gap (for $|\omega| > \Delta$) both $\tilde{\omega}$ and $\tilde{\Gamma}_S$ become complex quantities.

In what follows, we discuss the variation of the effective quasiparticle spectra with respect to the coupling Γ_S and magnetic field. The spectral function of spin-$\uparrow$ electrons is defined by

$$\rho_\uparrow(\omega) \equiv -\frac{1}{\pi}\mathrm{Im}\left\{\boldsymbol{G}(\omega + i0^+)\right\}_{11} \tag{11}$$

and $\rho_\downarrow(\omega)$ can be obtained in the same way by inverting the spin indices in the matrix Green's function (8).

2.1. Bound states of an unpolarized quantum dot

In the absence of magnetic polarization, the energy levels of the two-spin projections are equal, $\varepsilon_\uparrow = \varepsilon_\downarrow \equiv \varepsilon_d$. In the subgap regime, the Green's function (8) exhibits two poles at $\omega = \pm E_A$, which are determined by the solutions of the nonlinear equation

$$E_A\left(1 + \frac{\Gamma_S}{2}\frac{1}{\sqrt{\Delta^2 - E_A^2}}\right) = \pm\sqrt{\varepsilon_d^2 + \left(\frac{\Gamma_S}{2}\right)^2 \frac{\Delta^2}{\Delta^2 - E_A^2}}\,. \tag{12}$$

Figure 1 shows the spectral function $\rho_\sigma(\omega)$ of the unpolarized and uncorrelated quantum dot computed numerically for $\varepsilon_d = 0$. Its variation against the ratio Γ_S/Δ reveals the bound states near the gap edge singularities when the quantum dot is strongly hybridized with the superconducting host ($\Gamma_S \gg \Delta$). In contrast, the bound states move toward the interior of the pairing gap when the quantum dot is weakly coupled to the superconductor. These unpolarized in-gap quasiparticles are dubbed *Andreev states* due to the fact that any charge transfer via the subgap region is possible solely by converting an electron into a hole (initially discussed by Andreev), which engages both of the quasiparticle states at $\pm E_A$.

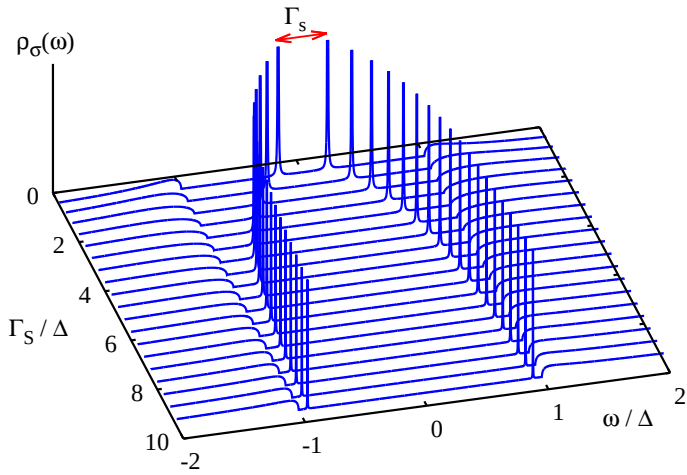

Fig. 1. Spectral function $\rho_\sigma(\omega)$ of the unpolarized quantum dot obtained for $\varepsilon_{\rm d}=0$, neglecting the correlations ($U=0$). In the strong coupling limit, $\Gamma_{\rm S}\gg\Delta$, the bound states show up near the gap edge singularities $\pm\Delta$. They gradually move towards the central subgap region in the weakly coupled regime, when $\Gamma_{\rm S}\leq\Delta$.

In the weak-coupling regime, $\Gamma_{\rm S}\lesssim\Delta$, where $E_A^2\ll\Delta^2$, one can assume $\omega\ll\Delta$. In this limit, the self-energy (6) simplifies to a static form

$$\boldsymbol{\Sigma}^0(\omega)=-\begin{pmatrix} 0 & \frac{\Gamma_{\rm S}}{2} \\ \frac{\Gamma_{\rm S}}{2} & 0 \end{pmatrix}. \tag{13}$$

In this regime, the proximity effect induces an effective on-site pairing amplitude $\Gamma_{\rm S}/2$ on the quantum dot. The resulting Andreev bound-state energies are given by $\pm\sqrt{\varepsilon_{\rm d}^2+(\Gamma_{\rm S}/2)^2}$. The subgap spectral function $\rho_\sigma(\omega)$ then simplifies to the familiar BCS-type form

$$\rho_\sigma(\omega)=\frac{1}{2}\left[1+\frac{\varepsilon_{\rm d}}{E_A}\right]\delta(\omega-E_A)+\frac{1}{2}\left[1-\frac{\varepsilon_{\rm d}}{E_A}\right]\delta(\omega+E_A)\,. \tag{14}$$

The subgap spectrum consists of two quasiparticle peaks symmetrically spaced with respect to the Fermi level of the superconductor $\mu_{\rm S}\equiv 0$, whose spectral weights can differ, depending on the energy level $\varepsilon_{\rm d}$.

2.2. Polarized bound states

Let us now consider the polarized quantum dot, for instance, induced by an external magnetic field which splits the energy levels

$$\varepsilon_\uparrow=\varepsilon_{\rm d}-\frac{1}{2}B_z\,,\qquad \varepsilon_\downarrow=\varepsilon_{\rm d}+\frac{1}{2}B_z \tag{15}$$

by the Zeeman energy B_z. To some extent, this situation mimics the magnetic impurities (such as Fe, Co) which are known to be detrimental to s-wave superconductors [1]. Here, we analyze the single impurity, therefore, its influence on the macroscopic superconductor is negligible. We focus instead on the quasiparticle spectrum of this polarized quantum impurity, paying special attention to the subgap region.

Figure 2 displays the typical variation of the spectral functions $\rho_\uparrow(\omega)$ and $\rho_\downarrow(\omega)$ against the Zeeman energy B_z. We notice that the in-gap states of different spin sectors are shifted — for a weak magnetic field roughly by B_z. With further increase of B_z, a pair of the outer bound states approaches the gap edges $\pm\Delta$. The other (inner) pair of the bound states is symmetrically located with respect to the Fermi level μ_S. Let us note that these inner bound states are fully polarized. These YSR states were initially predicted for classical magnetic impurities in bulk superconductors [27]. Their role in various superconducting nanostructures is presently often considered for the realization of topologically nontrivial superconducting phases [10].

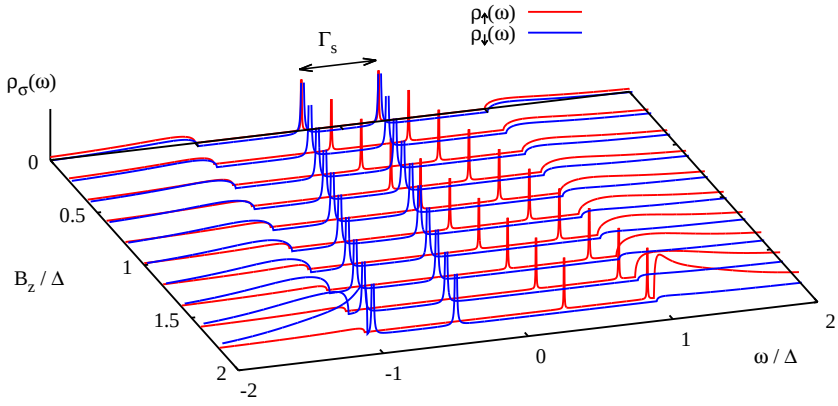

Fig. 2. The spectral functions $\rho_\sigma(\omega)$ obtained for $\sigma =\uparrow$ (blue) and $\sigma =\downarrow$ (red) electrons, using the model parameters $U = 0$, $\Gamma_S = 0.7\Delta$, $\varepsilon_d = 0$.

2.3. Correlation effects

The subgap spectrum is strongly influenced by electron–electron interactions, when present. In a single quantum dot coupled to a superconductor, the on-site Coulomb repulsion U competes with the proximity-induced pairing. As a result, the energies of the subgap states depend significantly on U, Γ_S, as well as ε_d. At a critical interaction strength U_c, determined by these parameters, the subgap excitations cross at zero energy, signaling a quantum

phase transition between ground states of different parity. For $U < U_c$, the system is in an even-parity many-body singlet state, whereas for $U > U_c$, it transitions to an odd-parity doublet configuration [28, 29].

The singlet phase itself comprises two distinct regimes. For weak and moderate interactions, $U \lesssim \Delta, \Gamma_S$, the ground state has a BCS-like character, *i.e.*, it forms a coherent superposition of the empty and doubly occupied states $u|0\rangle - v|\uparrow\downarrow\rangle$. In contrast, for $\Delta \ll U < U_c$, the singlet acquires a Kondo-like character, resulting from the screening of the localized spin by the Kondo cloud [30].

For multi-dot systems, the enlarged parameter space leads to a richer subgap spectrum and more intricate phase diagrams [31–33]. The inter-dot Coulomb (capacitive) interactions may further reshape the in-gap states [34, 35], although a detailed analysis of these effects lies beyond the scope of the present work.

3. Molecular bound states

Numerous recent studies have explored the bound states of multi-dot structures hybridized with superconducting reservoirs. Inter-dot (lateral) coupling modifies the individual in-gap states, leading to the formation of a more complex *molecular*-like spectrum. Here, we address this problem in the simplest, yet nontrivial, setting of a double quantum dot. Two quantum dots proximitized by a superconducting reservoir have attracted considerable attention due to their potential realization of a minimal Kitaev chain supporting Majorana quasiparticles [18–20, 36].

Specifically, we consider the hybrid system consisting of two quantum dots coupled on one side to the superconductor and on the opposite side to the metallic lead. This setup can be described by the Hamiltonian

$$\hat{H} = \hat{H}_S + \hat{H}_{S-QD_1} + \hat{H}_{QD_1} + \hat{H}_{QD_1-QD_2} + \hat{H}_{QD_2} + \hat{H}_{N-QD_2} + \hat{H}_N\,, \quad (16)$$

where we treat the quantum dots as Anderson-type impurities $\hat{H}_{QD_i} = \sum_\sigma \varepsilon_{i\sigma}\hat{n}_{i,\sigma} + U_i\,\hat{n}_{i,\uparrow}\hat{n}_{i,\downarrow}$, their hybridization with external leads is expressed in the same way as in Eq. (2), and the inter-dot coupling is

$$\hat{H}_{QD_1-QD_2} = t_{12}\sum_\sigma \left(\hat{d}^\dagger_{1,\sigma}\hat{d}_{2,\sigma} + \hat{d}^\dagger_{2,\sigma}\hat{d}_{1,\sigma}\right). \quad (17)$$

The normal lead is described as a free fermion gas $\hat{H}_N = \sum_{\boldsymbol{k},\sigma}\xi_{\boldsymbol{k}N}\hat{c}^\dagger_{\boldsymbol{k}\sigma N}\hat{c}_{\boldsymbol{k}\sigma N}$ and is regarded as a probing electrode for tunneling measurements. For this reason, the coupling $\Gamma_N = 2\pi\sum_{\boldsymbol{k}}|V_{\boldsymbol{k}N}|^2\delta(\omega - \xi_{\boldsymbol{k}N})$ is assumed to be much smaller than Γ_S.

Let us investigate the uncorrelated case, $U_i = 0$, when the quasiparticle spectra of both quantum dots can be determined exactly. We use again the matrix Green's functions $\boldsymbol{G}_i(\tau,\tau') = \langle\langle \hat{\Psi}_i(\tau); \hat{\Psi}_i^\dagger(\tau')\rangle\rangle$ in the Nambu representation $\hat{\Psi}_i^\dagger = (\hat{d}_{i,\uparrow}^\dagger, \hat{d}_{i,\downarrow})$, $\hat{\Psi}_i = (\hat{\Psi}_i^\dagger)^\dagger$. The matrix Green's functions are coupled through the set of equations

$$\boldsymbol{G}_1(\omega)^{-1} = \begin{pmatrix} \omega-\varepsilon_{1\uparrow} & 0 \\ 0 & \omega+\varepsilon_{1\downarrow} \end{pmatrix} + \frac{\gamma(\omega)\Gamma_\mathrm{S}}{2} \begin{pmatrix} 1 & \frac{\Delta}{\omega} \\ \frac{\Delta}{\omega} & 1 \end{pmatrix} - (t_{12})^2\, \boldsymbol{G}_2(\omega)\,, \tag{18}$$

$$\boldsymbol{G}_2(\omega)^{-1} = \begin{pmatrix} \omega-\varepsilon_{2\uparrow} & 0 \\ 0 & \omega+\varepsilon_{2\downarrow} \end{pmatrix} + \frac{i\Gamma_\mathrm{N}}{2} \begin{pmatrix} 1 & 0 \\ 0 & 1 \end{pmatrix} - (t_{12})^2\, \boldsymbol{G}_1(\omega)\,. \tag{19}$$

The lowest order estimation of the matrix Green's function of QD_1 yields

$$\boldsymbol{G}_1(\omega) \approx \begin{pmatrix} \omega-\varepsilon_{1\uparrow} + \frac{\Gamma_\mathrm{S}}{2}\gamma(\omega) - \frac{t_{12}^2}{\omega-\varepsilon_{2\uparrow}+i\Gamma_\mathrm{N}/2} & \frac{\Gamma_\mathrm{S}\Delta}{2\omega}\gamma(\omega) \\ \frac{\Gamma_\mathrm{S}\Delta}{2\omega}\gamma(\omega) & \omega+\varepsilon_{1\downarrow} + \frac{\Gamma_\mathrm{S}}{2}\gamma(\omega) - \frac{t_{12}^2}{\omega+\varepsilon_{2\downarrow}+i\Gamma_\mathrm{N}/2} \end{pmatrix}^{-1} \tag{20}$$

and by inserting it into Eq. (19), one can determine the first estimation for the Green's function $\boldsymbol{G}_2(\omega)$. Next, the matrix functions can be iteratively updated, until numerical convergence is reached.

Figure 3 shows the molecular spectrum $\rho_{1\sigma}(\omega)$, varying as a function of the energy level $\varepsilon_{2\sigma}$. We can clearly recognize the features inherited from the proximitized QD_1 (*i.e.* two in-gap states, roughly spaced by Γ_S) and additional structures appearing around $\pm\varepsilon_{2\sigma}$ contributed by electronic states of QD_2. In the latter case, we notice the particle and hole components which arise from the electron pairing transmitted to QD_2 from QD_1 through the inter-dot coupling t_{12}. The optimal condition for this pairing $\langle \hat{d}_{2\downarrow}\hat{d}_{2\uparrow}\rangle$ occurs when the energy level $\varepsilon_{2\sigma}$ approaches μ_S. This is manifested by the quasiparticle peaks at $\sim \pm\varepsilon_{2\sigma}$ whose spectral weights are sensitive to $\varepsilon_{2\sigma}$. The initial bound states of QD_1 slightly change their energies as well, revealing an avoided-crossing behavior. Effectively, for $\varepsilon_{2\sigma} \to \mu_\mathrm{S}$, the subgap spectrum consists of four quasiparticle peaks. Such *molecular Andreev bound states* have been detected experimentally in a variety of systems [22–25].

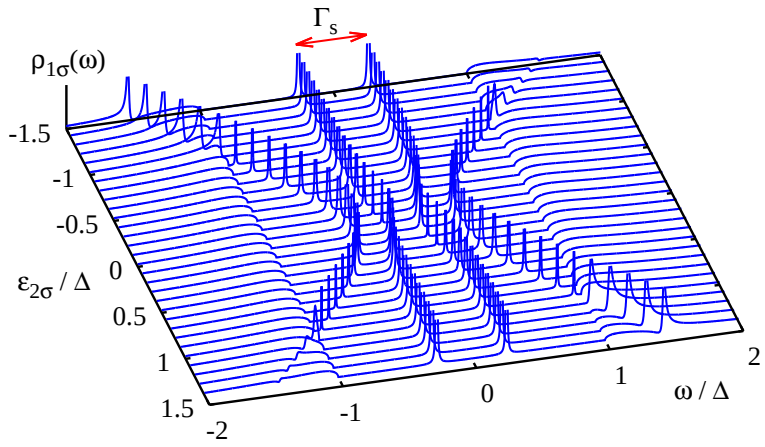

Fig. 3. Variation of the spectral functions $\rho_{1\sigma}(\omega)$ against $\varepsilon_{2\sigma}$ obtained for the uncorrelated quantum dots ($U_i = 0$), using the model parameters $\Gamma_S = 0.7\Delta$, $\varepsilon_{1\sigma} = 0$, $t_{12} = 0.25\Delta$.

3.1. Influence of magnetic field

Double quantum dots proximitized by a superconductor have attracted considerable attention, partly due to their potential applications in superconducting qubit architectures [37, 38]. Their properties can be probed experimentally via charge transport. In the subgap regime (where voltage is much lower than Δ), the current is predominantly mediated by the Andreev/YSR processes, involving coherent electron-to-hole conversion at the superconducting interface. Such processes rely on induced pairing correlations within the quantum dots. If the on-dot pairing amplitude is suppressed, for instance, due to strong Coulomb repulsion competing with the proximity effect, the subgap transport can become strongly reduced or even blocked [39]. This type of blockade has been experimentally observed in the S–QD_1–QD_2–N junctions [40] as well as in the Josephson-type S–QD_1–QD_2–S geometries [41].

We propose here an alternative mechanism leading to an analogous blockade effect, originating from an external magnetic field which, through the Zeeman splitting of the quantum-dot levels (15), suppresses the on-dot pairing correlations. We demonstrate how this suppression emerges in a quench scenario, where the magnetic field is abruptly switched from zero to a finite value.

Specifically, we assume as the initial condition that the dot levels $\varepsilon_{i\sigma}$ are spin-degenerate and aligned with the Fermi level of the external leads. At time $t \geq 0$, the magnetic field is suddenly turned on, resulting in a Zeeman splitting of the energy levels

$$\varepsilon_{i\downarrow} - \varepsilon_{i\uparrow} = \begin{cases} 0 & \text{for} \quad t \leq 0\,, \\ B_z & \text{for} \quad t > 0\,. \end{cases} \tag{21}$$

To analyze this nonequilibrium dynamics, we employ the recently introduced chain expansion (ChE) technique [33], which enables access to the full time evolution of the hybrid system up to the steady state by mapping the superconducting and normal-metal leads onto effective tight-binding chains using a Padé expansion.

In Fig. 4, we present the post-quench expectation values of the dot occupancies, $n_{i\sigma}(t) = \langle \hat{d}^\dagger_{i\sigma}(t)\hat{d}_{i\sigma}(t)\rangle$, for both spin projections. The results correspond to the weak-coupling regime $\Gamma_\mathrm{S} = 0.02\Delta$, where the initial bound states are located at $\pm\Gamma_\mathrm{S}/2$ and the dots are spin-degenerate, $n_{i\uparrow} = n_{i\downarrow}$. Following the quench, a spin polarization gradually develops in an oscillatory manner on both dots. In the long-time limit, each dot becomes predominantly occupied by a single $\uparrow$-spin electron.

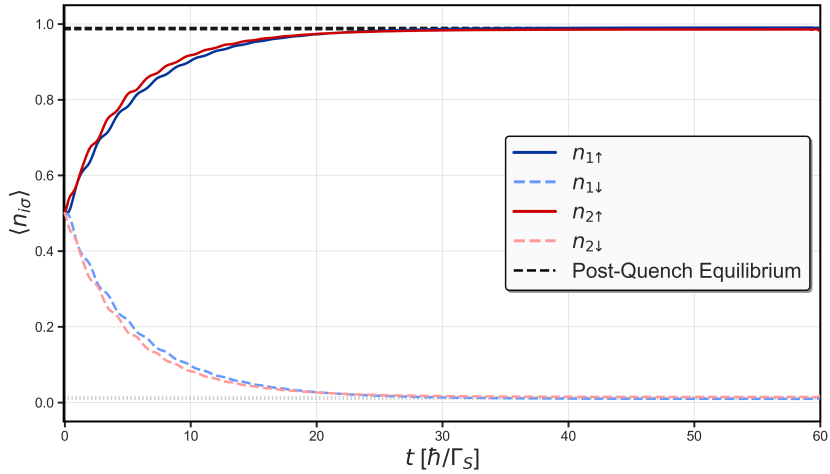

Fig. 4. Time-dependent occupancy of the quantum dots, $n_{i\sigma}(t)$, following the magnetic-field quench at $t = 0$ from $B_z = 0$ to $B_z = \frac{1}{5}\Delta$. The results correspond to uncorrelated dots ($U_i = 0$) and parameters $\Gamma_\mathrm{S} = \frac{1}{50}\Delta$, $t_{12} = 2\Gamma_\mathrm{S}$, $\Gamma_\mathrm{N} = 0.2\Gamma_\mathrm{S}$, with $\varepsilon_{i\downarrow}(t > 0) = \frac{1}{2}B_z$ and $\varepsilon_{i\uparrow}(t > 0) = -\frac{1}{2}B_z$. The dashed horizontal lines indicate the steady-state, respective, post-quench equilibrium values at $B_z = \frac{1}{5}\Delta$.

The gradual formation of the triplet configuration is accompanied by a pronounced suppression of the superconducting on-dot pairing correlations, as shown in Fig. 5. At $t = 0$, both dots exhibit substantial induced pairing, with a slightly smaller amplitude on the dot coupled to the normal lead, as expected from the reduced SC proximity effect. Following the quench, the strong magnetic field rapidly suppresses the BCS singlet correlations that were present on both quantum dots.

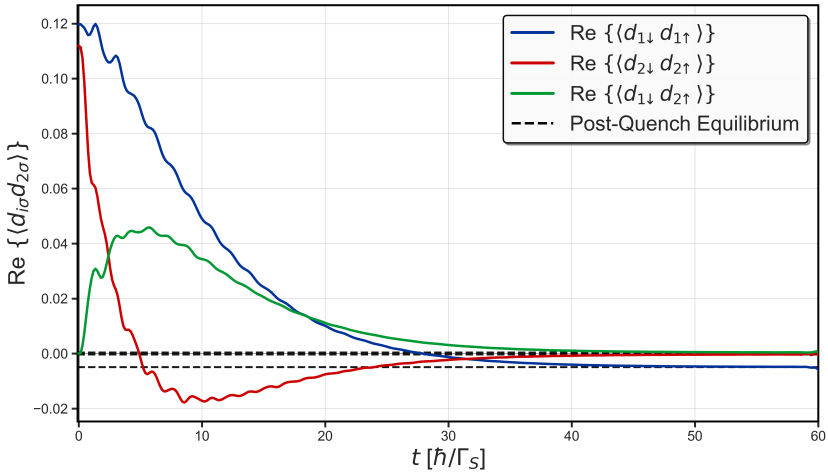

Fig. 5. Time-dependence of the on-dot pairings $\langle \hat{d}_{i\downarrow}\hat{d}_{i\uparrow}\rangle$ (blue and red curves) and inter-dot pairing $\langle \hat{d}_{1\downarrow}\hat{d}_{2\uparrow}\rangle$ induced by the quench in magnetic field from $B_z(t\leq 0)=0$ to $B_z(t>0)=\frac{1}{5}\Delta$. Numerical results are obtained for the uncorrelated quantum dots, $U_i=0$, using the model parameters $\Gamma_{\rm S}=\frac{1}{50}\Delta$, $t_{12}=2\Gamma_{\rm S}$, $\Gamma_{\rm N}=0.2\Gamma_{\rm S}$ and $\varepsilon_{i\downarrow}(t>0)=\frac{1}{2}B_z$, $\varepsilon_{i\uparrow}(t>0)=-\frac{1}{2}B_z$. The imaginary parts are zero.

The dot directly coupled to the superconducting reservoir (QD_1) retains a finite residual pairing amplitude in the long-time limit, albeit with reversed sign. This finite anomalous expectation value reflects the proximity effect mediated by virtual tunneling processes between the dot and the superconducting condensate. Even in the presence of Zeeman splitting, such virtual processes generate remnant pairing correlations through the hybridization with the gapped quasiparticle spectrum of the reservoir. Microscopically, this behavior is closely related to the formation of YSR bound states induced by magnetic perturbations in a superconducting host [8, 10].

In contrast, the second dot (QD_2), which is only indirectly coupled to the superconductor, exhibits an almost complete suppression of pairing correlations in the long-time limit, $\lim_{t\to\infty}\langle \hat{d}_{2\downarrow}\hat{d}_{2\uparrow}\rangle \approx 0$. Since the proximity effect on QD_2 is mediated solely via inter-dot coupling, the induced anomalous correlations are strongly suppressed by the Zeeman splitting. Although the post-quench dynamics initially generates a finite inter-dot pairing amplitude (green line in Fig. 5), it rapidly decays at longer times as well.

Consequently, in this regime, the subgap transport ($e|V|\leq\Delta$) becomes strongly suppressed, as the Andreev transmission channel requires coherent pairing either locally on QD_2 or between the dots. In their absence, the conversion of electrons into Cooper pairs is effectively blocked.

3.2. Triplet inter-dot pairing

We have shown that the magnetic field is detrimental to the on-dot pairing of opposite-spin electrons. In contrast, in the presence of spin-mixing mechanisms, it can promote the emergence of inter-dot triplet correlations between electrons residing on neighboring quantum dots. Similarly, in bulk materials, the local spin-triplet pairing can be induced among fermions by ferromagnetic exchange, for example, originating from the Hund's rule coupling [42]. Such a mechanism of triplet pairing has been discussed in the literature as a possible route toward realizing a minimal (two-site) Kitaev chain [43]. Generation of equal-spin inter-dot pairing requires spin-reversal (spin-flip) tunneling between the dots. This can be achieved, for instance, by coupling the proximitized double quantum dot system to a semiconductor with the strong Rashba spin–orbit interaction [18–20]. Alternatively, similar physics may arise in the Cooper pair splitter geometries [36] employing spin-selective filtering side gates [17].

Here, we show, as a proof of principle, that our setup of two quantum dots embedded in series between the superconductor and the normal lead can support the equal-spin inter-dot pairing. For this purpose, we amend the model Hamiltonian, Eq. (16), by the spin-reversal hopping term

$$\hat{H}_{\mathrm{SOC}} = t_{12}\left(\hat{d}^{\dagger}_{1\uparrow}\hat{d}_{2\downarrow} - \hat{d}^{\dagger}_{1\downarrow}\hat{d}_{2\uparrow} + \hat{d}^{\dagger}_{2\downarrow}\hat{d}_{1\uparrow} - \hat{d}^{\dagger}_{2\uparrow}\hat{d}_{1\downarrow}\right). \tag{22}$$

Following the procedure discussed by us in Ref. [44], we computed the time-dependent electron pairings in various spin channels, assuming that all components of the S–QD_1–QD_2–N setup are abruptly contacted at $t = 0$.

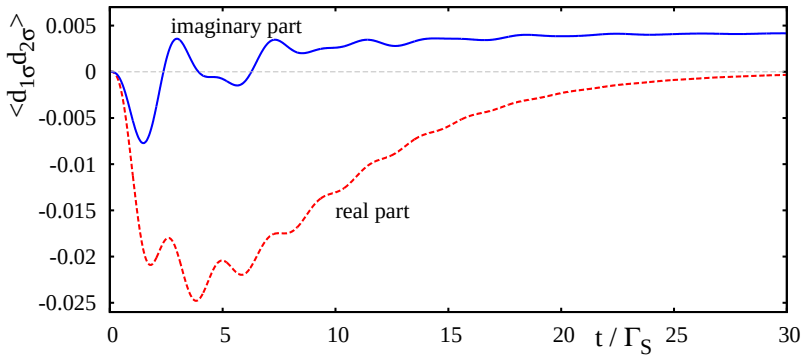

Fig. 6. Time-dependent buildup of the inter-dot triplet pairing $\langle \hat{d}_{1\sigma}\hat{d}_{2\sigma}\rangle$ for $\sigma = \uparrow$ electrons, assuming that components of the S–QD_1–QD_2–N junction are coupled at $t = 0$. Numerical results are obtained for the uncorrelated quantum dots in the large pairing gap limit, $\Delta \gg \Gamma_{\mathrm{S}}$, using the model parameters $\Gamma_{\mathrm{N}} = 0.5\Gamma_{\mathrm{S}}$, $t_{12} = \Gamma_{\mathrm{S}}$, $\varepsilon_{i\sigma} = 0$, and $t_{\mathrm{SOC}} = 1\Gamma_{\mathrm{S}}$.

For brevity, we concentrate on the triplet pairing of ↑-spin electrons and in Fig. 6 we show the results obtained for the uncorrelated quantum dots, assuming identical magnitude of the hopping processes without and with the spin reversal. We notice that the complex pairing function $\langle \hat{d}_{1\uparrow}\hat{d}_{2\uparrow}\rangle$ evolves to the purely imaginary value. Its finite absolute value is necessary for the emergence of the zero-energy boundary modes, provided that the set of *sweet spot* parameters can be satisfied [20]. Such a requirement within the presently considered model is rather challenging, and its feasibility will be discussed in more detail separately.

4. Summary

We have investigated the quasiparticle states of single and double quantum dots hybridized with a conventional superconductor. Due to hybridization with the superconducting reservoir, subgap bound states emerge in the dot spectrum, reflecting the electron–hole mixing induced by the proximity effect. In the weak-coupling regime, these states appear well inside the pairing gap, centered around the chemical potential $\mu_{\rm S}$ of the superconductor. For strong hybridization, however, the bound states shift toward the gap edges $\pm\Delta$, rendering a nonmagnetic impurity nearly indistinguishable from the superconducting host, consistent with Anderson's theorem [1].

We have examined the evolution of these bound states under an external magnetic field, which induces the Zeeman splitting of the dot levels. The resulting subgap states become spin-polarized and shift in energy. In the strong-field regime, one pair approaches the gap edges, while the remaining in-gap states evolve into fully polarized quasiparticles, analogous to the Shiba states of classical magnetic impurities [8].

Extending the analysis to a double quantum dot coupled to a superconductor on one side and weakly to a metallic lead on the other, we demonstrated that both dots can acquire pairing correlations provided the energy level of the impurity coupled to the normal lead lies sufficiently close to $\mu_{\rm S}$. In this regime, the spectrum consists of two pairs of in-gap peaks forming *molecular Andreev* states. A magnetic field suppresses these proximity-induced correlations, and in a biased configuration, this suppression blocks charge transport mediated by electron–hole conversion.

Finally, we addressed triplet pairing induced between the dots by the Rashba-type spin–orbit interaction modeled through the spin-reversal hopping term (22). In the nonequilibrium transient regime, we observed the gradual emergence of a complex pairing amplitude, whose steady-state magnitude remains small as it arises as a higher-order effect of spin-mixing in already proximitized dots. Nevertheless, in alternative geometries, such as dots interconnected through a narrow superconductor [18–20] or embedded

in the Cooper pair splitter architectures [36], the triplet component can be substantially enhanced. Our results therefore provide a proof of principle that proximitized multi-dot systems with spin–orbit coupling can host triplet correlations, which under suitable parameter tuning may enable the realization of Majorana-type boundary modes.

T.D. acknowledges support by the National Science Centre (NCN), Poland within the Weave-Unisono grant No. 2022/04/Y/ST3/00061. L.S. and M.Ž. acknowledge support from the Czech Science Foundation through Project No. 23-05263K. L.S. further acknowledges support by the Charles University Grant Agency under project No. 512426.

REFERENCES

[1] P.W. Anderson, «Theory of dirty superconductors», *J. Phys. Chem. Solids* **11**, 26 (1959).

[2] J. Spałek, M. Fidrysiak, M. Zegrodnik, A. Biborski, «Superconductivity in high-T_c and related strongly correlated systems from variational perspective: Beyond mean field theory», *Phys. Rep.* **959**, 1 (2022).

[3] M.M. Maśka, Ż. Śledź, K. Czajka, M. Mierzejewski, «Inhomogeneity-Induced Enhancement of the Pairing Interaction in Cuprate Superconductors», *Phys. Rev. Lett.* **99**, 147006 (2007).

[4] B.W. Heinrich, J.L. Pascual, K.J. Franke, «Single magnetic adsorbates on *s*-wave superconductors», *Prog. Surf. Sci.* **93**, 1 (2018).

[5] Ø. Fischer, M. Kugler, I. Maggio-Aprile, C. Berthod, «Scanning tunneling spectroscopy of high-temperature superconductors», *Rev. Mod. Phys.* **79**, 353 (2007).

[6] S. Rachel, R. Wiesendanger, «Majorana quasiparticles in atomic spin chains on superconductors», *Phys. Rep.* **1099**, 1 (2025).

[7] H. Huang *et al.*, «Quantum phase transitions and the role of impurity-substrate hybridization in Yu–Shiba–Rusinov states», *Commun. Phys.* **3**, 199 (2020).

[8] A.V. Balatsky, I. Vekhter, J.-X. Zhu, «Impurity-induced states in conventional and unconventional superconductors», *Rev. Mod. Phys.* **78**, 373 (2006).

[9] A. Martín-Rodero, A. Levy-Yeyati, «Josephson and Andreev transport through quantum dots», *Adv. Phys.* **60**, 899 (2011).

[10] M. Pita-Vidal *et al.*, «Novel qubits in hybrid semiconductor-superconductor nanostructures», arXiv:2512.23336 [cond-mat.mes-hall].

[11] J.M. Martinis, M.H. Devoret, J. Clarke, «Quantum Josephson junction circuits and the dawn of artificial atoms», *Nat. Phys.* **16**, 234 (2020).

[12] M. Pita-Vidal, J.J. Wesdorp, C.K. Andersen, «Blueprint for All-to-All-Connected Superconducting Spin Qubits», *PRX Quantum* **6**, 010308 (2025).

[13] J. Bauer, A. Oguri, A.C. Hewson, «Spectral properties of locally correlated electrons in a Bardeen–Cooper–Schrieffer superconductor», *J. Phys.: Condens. Matter* **19**, 486211 (2007).

[14] R.S. Deacon *et al.*, «Kondo-enhanced Andreev transport in single self-assembled InAs quantum dots contacted with normal and superconducting leads», *Phys. Rev. B* **81**, 121308(R) (2010).

[15] J.-D. Pillet *et al.*, «Andreev bound states in supercurrent-carrying carbon nanotubes revealed», *Nat. Phys.* **6**, 965 (2010).

[16] V. Mourik *et al.*, «Signatures of Majorana Fermions in Hybrid Superconductor–Semiconductor Nanowire Devices», *Science* **336**, 1003 (2012).

[17] A. Bordoloi *et al.*, «Spin cross-correlation experiments in an electron entangler», *Nature* **612**, 454 (2022).

[18] A. Tsintzis, R.S. Souto, M. Leijnse, «Creating and detecting poor man's Majorana bound states in interacting quantum dots», *Phys. Rev. B* **106**, L201404 (2022).

[19] C.-X. Liu, G. Wang, T. Dvir, M. Wimmer, «Tunable Superconducting Coupling of Quantum Dots via Andreev Bound States in Semiconductor–Superconductor Nanowires», *Phys. Rev. Lett.* **129**, 267701 (2022).

[20] M. Luethi, H.F. Legg, D. Loss, J. Klinovaja, «From perfect to imperfect poor man's Majoranas in minimal Kitaev chains», *Phys. Rev. B* **110**, 245412 (2024).

[21] P. Ram, D. Beckmann, R. Danneau, W. Belzig, «Multiterminal Josephson junctions with tunable topological properties», *Phys. Rev. B* **112**, 214508 (2025).

[22] L.M. Rütten *et al.*, «Wave Function Engineering on Superconducting Substrates: Chiral Yu–Shiba–Rusinov Molecules», *ACS Nano* **18**, 30798 (2024).

[23] S. Matsuo *et al.*, «Phase-dependent Andreev molecules and superconducting gap closing in coherently-coupled Josephson junctions», *Nat. Commun.* **14**, 8271 (2023).

[24] M. Kocsis *et al.*, «Strong nonlocal tuning of the current-phase relation of a quantum dot based Andreev molecule», *Phys. Rev. B* **109**, 245133 (2024).

[25] D. van Driel *et al.*, «Charge Sensing the Parity of an Andreev Molecule», *PRX Quantum* **5**, 020301 (2024).

[26] J. Barański, T. Domański, «In-gap states of a quantum dot coupled between a normal and a superconducting lead», *J. Phys.: Condens. Matter* **25**, 435305 (2013).

[27] Yu Luh, «Bound State in Superconductors with Paramagnetic Impurities», *Acta Phys. Sin.* **21**, 75 (1965); H. Shiba, «Classical Spins in Superconductors», *Prog. Theor. Phys.* **40**, 435 (1968); A.I. Rusinov, «On the theory of Gapless Superconductivity in Alloys with Paramagnetic Impurities», *Sov. Phys. JETP* **29**, 1101 (1969) [*Zh. Eksp. Theor. Phys.* **56**, 2047 (1969)]; H. Shiba, T. Soda, «Superconducting Tunneling through the Barrier with Paramagnetic Impurities», *Prog. Theor. Phys.* **41**, 25 (1969).

[28] V. Meden, «The Anderson–Josephson quantum dot — a theory perspective», *J. Phys.: Condens. Matter* **31**, 163001 (2019).

[29] A. Kadlecová, M. Žonda, V. Pokorný, T. Novotný, «Practical Guide to Quantum Phase Transitions in Quantum-Dot-Based Tunable Josephson Junctions», *Phys. Rev. Appl.* **11**, 044094 (2019).

[30] C.P. Moca, I. Weymann, M.A. Werner, G. Zaránd, «Kondo Cloud in a Superconductor», *Phys. Rev. Lett.* **127**, 186804 (2021).

[31] M. Žonda *et al.*, «Generalized atomic limit of a double quantum dot coupled to superconducting leads», *Phys. Rev. B* **107**, 115407 (2023).

[32] P. Zalom, K. Wrześniewski, T. Novotný, I. Weymann, «Double quantum dot Andreev molecules: Phase diagrams and critical evaluation of effective models», *Phys. Rev. B* **110**, 134506 (2024).

[33] D. Bobok, L. Frk, V. Pokorný, M. Žonda, «Scalable effective models for superconducting nanostructures: Applications to double, triple, and quadruple quantum dots», *Phys. Rev. B* **112**, 205418 (2025).

[34] C. Li *et al.*, «Individual Assembly of Radical Molecules on Superconductors: Demonstrating Quantum Spin Behavior and Bistable Charge Rearrangement», *ACS Nano* **19**, 3403 (2025).

[35] C. Li *et al.*, «Negative differential conductance in triangular molecular assemblies», arXiv:2508.05575 [cond-mat.mes-hall].

[36] B.R. Bułka, T. Domański, K.I. Wysokiński, «Interplay of spin-orbit interaction and Andreev reflection in proximized quantum dots», *Phys. Rev. B* **113**, 115430 (2026), arXiv:2510.17379 [cond-mat.mes-hall].

[37] M. Geier *et al.*, «Fermion-parity qubit in a proximitized double quantum dot», *Phys. Rev. Res.* **6**, 023281 (2024).

[38] G.O. Steffensen, A.L. Yeyati, «Yu–Shiba–Rusinov-Bond Qubit in a Double Quantum Dot with Circuit-QED Operation», *PRX Quantum* **6**, 020329 (2025).

[39] Z. Scherübl, A. Pályi, S. Csonka, «Transport signatures of an Andreev molecule in a quantum dot–superconductor–quantum dot setup», *Beilstein J. Nanotechnol.* **10**, 363 (2019).

[40] P. Zhang *et al.*, «Signatures of Andreev Blockade in a Double Quantum Dot Coupled to a Superconductor», *Phys. Rev. Lett.* **128**, 046801 (2022).

[41] D. Bouman *et al.*, «Triplet-blockaded Josephson supercurrent in double quantum dots», *Phys. Rev. B* **102**, 220505 (2020).

[42] J. Spałek, «Spin-triplet superconducting pairing due to local Hund's rule and Dirac exchange», *Phys. Rev. B* **63**, 104513 (2001).

[43] T. Dvir *et al.*, «Realization of a minimal Kitaev chain in coupled quantum dots», *Nature* **614**, 445 (2023).

[44] R. Taranko *et al.*, «Transient effects in a double quantum dot sandwiched laterally between superconducting and metallic leads», *Phys. Rev. B* **103**, 165430 (2021).